AGU PUBLICATIONS

Geophysical Research Letters

RESEARCH LETTER
10.1002/2014GL062133

Disruption and reaccretion of midsized moons during an outer solar system Late Heavy Bombardment

N. Movshovitz[1], F. Nimmo[1], D. G. Korycansky[1], E. Asphaug[2], and J. M. Owen[3]

[1]Department of Earth and Planetary Sciences, University of California, Santa Cruz, California, USA, [2]School of Earth and Space Exploration, Arizona State University, Tempe, Arizona, USA, [3]Lawrence Livermore National Laboratory, Livermore, California, USA

Key Points:
- Midsized moons disrupt and reaccrete multiple times during an LHB
- The surfaces of these moons cannot record any event prior to 3.9 Ga
- Mimas must have reaccreted undifferentiated

Supporting Information:
- Figure S1
- Text S1
- Figure S2

Correspondence to:
N. Movshovitz,
nmovshov@ucsc.edu

Citation:
Movshovitz, N., F. Nimmo, D. G. Korycansky, E. Asphaug, and J. M. Owen (2015), Disruption and reaccretion of midsized moons during an outer solar system Late Heavy Bombardment, *Geophys. Res. Lett.*, *42*, doi:10.1002/2014GL062133.

Received 6 OCT 2014
Accepted 19 DEC 2014
Accepted article online 23 DEC 2014

Abstract We investigate the problem of satellite survival during a hypothetical Late Heavy Bombardment in the outer solar system, as predicted by the Nice model (Tsiganis, Gomes, Morbidelli, and Levison 2005, Nature 435). Using a Monte Carlo approach we calculate, for satellites of Jupiter, Saturn, and Uranus, the probability of experiencing a catastrophic collision during the Late Heavy Bombardment (LHB). We find that Mimas, Enceladus, Tethys, and Miranda experience at least one catastrophic impact in every simulation. Because reaccretion is expected to be rapid, these bodies will have emerged as scrambled mixtures of rock and ice. Tidal heating may have subsequently modified the latter three, but in the nominal LHB model Mimas should be a largely undifferentiated, homogeneous body. A differentiated Mimas would imply either that this body formed late or that the Nice model requires significant modification.

1. Introduction

The lunar Late Heavy Bombardment (LHB; the apparent clustering of lunar basin ages around 3.9 Ga) can be explained by a model [*Tsiganis et al.*, 2005; *Gomes et al.*, 2005] that invokes a period of dynamical instability occurring long after planet formation. In this model, often called the Nice model, the giant planets are formed in circular orbits, all inside of 20 AU, while an exterior disk of unaccreted planetesimals remains beyond 30 AU. Scattering of planetesimals due to chance encounters results in slow migration of the giant planets until Jupiter and Saturn reach a 1:2 mean motion resonance. The resulting dynamical instability destabilizes both the asteroid main belt and the exterior planetesimal disk. A careful choice of initial conditions can delay the onset of instability to about 700 My after planet formation, delivering enough planetesimal mass to the Earth-Moon system at 3.9 Ga to cause the lunar LHB [*Gomes et al.*, 2005].

The above scenario also predicts an LHB-like period in the outer solar system. In fact, the higher-collision probabilities and impact energies due to gravitational focusing by the giant planets suggest that the inner satellites of Jupiter, Saturn, and Uranus would have experienced a bombardment much more severe than the one supposedly responsible for the lunar basins. The concern is that this outer solar system LHB should have resulted not just in cratering, but in significant, even catastrophic modification of the smaller satellites [e.g., *Barr and Canup*, 2010; *Nimmo and Korycansky*, 2012]. The general vulnerability of the smaller satellites to catastrophic disruption and reaccretion has been noted by previous authors [e.g., *Smith et al.*, 1982, 1986; *Zahnle et al.*, 2003], and the probability of satellite survival in the context of the proposed 3.9 Ga LHB was also calculated in *Charnoz et al.* [2009]. Our contribution is to examine in detail the expected level of destruction experienced by each satellite.

In a previous study *Nimmo and Korycansky* [2012] have shown, using estimates of impactor populations [*Charnoz et al.*, 2009], collision probabilities [*Zahnle et al.*, 2003], and a scaling law for impact-induced vapor production [*Kraus et al.*, 2011], that several satellites (Mimas, Enceladus, and Miranda) should have lost most of their ice content during the LHB, unless the total mass delivered to the outer solar system was a factor of 10 smaller than predicted by the original Nice model [*Barr and Canup*, 2010; *Dones and Levison*, 2013].

In this work we look again at the problem of satellite survival, this time focusing on disruption rather than vaporization. We calculate the probability of a satellite experiencing one or more impacts energetic enough to disperse more than 50% of the target's mass (not necessarily vaporized). We find that disruption is much more dangerous than vaporization, particularly for the inner satellites of Saturn. In fact, it seems very unlikely that these satellites could have survived the nominal LHB unmodified in their present orbits.

2. Method

For each satellite of interest we ask: What is the probability of it suffering at least one *catastrophic* collision, defined as a collision that disperses at least half the original target mass, during a hypothetical LHB? To answer this question, we need to know the total mass of impactors delivered to the target satellite, the statistics of the impactor population (in particular, the size and velocity distribution of impacting bodies), and the effects of a given impact. We consider each of these elements in turn in the following sections and then describe how they are used in a Monte Carlo simulation of an outer solar system LHB.

2.1. Total Mass of Impactors Delivered to Each Target

The Nice model explanation for the lunar LHB requires a rather massive planetesimal disk external to the orbits of the giant planets. *Gomes et al.* [2005] suggest 35 Earth masses (M_{E}) in the initial disk. From the output of these simulations, several authors estimate the mass expected to strike Saturn between 0.06 and 0.37 M_{E} [*Charnoz et al.*, 2009; *Barr and Canup*, 2010; *Dones and Levison*, 2013]. Later studies have suggested ways of reducing somewhat the predicted disk mass [e.g., *Nesvorný*, 2011; *Nesvorný et al.*, 2013]. In this work we treat the total delivered mass as a free parameter, spanning the range suggested by previous studies and down to less than 1% of the canonical value.

The mass delivered to each satellite of interest is calculated based on the relative impact probabilities given by *Zahnle et al.* [2003, Table 1]. *Zahnle et al.* [2003] report impact probabilities relative to Jupiter, $P_{\mathrm{EC}}^{\mathrm{sat}}$. We denote by M_{LHB} the total mass delivered to Jupiter, and thus $M_{\mathrm{LHB}}^{\mathrm{sat}} = P_{\mathrm{EC}}^{\mathrm{sat}} M_{\mathrm{LHB}}$. A satellite's relative probability of being hit scales with the square of its radius and inversely with its orbital distance (assuming an approximately circular orbit and strong gravitational focusing by the primary).

2.2. Mass Dispersed by an Impact

An impact is characterized by the target's mass M and radius R, the impactor's mass m_i and radius r_i, and the impact velocity v_i (in the target's rest frame) and angle θ. We are interested in the gravity regime where material strength may be ignored. For a given target, and for impacts in the near-catastrophic regime, it is customary to make the assumption that the outcome is determined by the specific impact energy $Q = (m_i v_i^2)/(2M)$. More precisely, numerical simulations [*Benz and Asphaug*, 1999; *Leinhardt and Stewart*, 2012] show that for a given target, the fraction of target mass that remains bound in the largest postcollision fragment is a linear function of Q:

$$\frac{M_{lr}}{M} = \max\left(0, 1 - 0.5\frac{Q}{Q_D^*}\right). \tag{1}$$

The parameter Q_D^* is the specific energy required to disperse half the target mass and is a function of the target radius.

In this work we are interested in targets in the 100 to 1000 km range. To extend previous scaling laws for $Q_D^*(R)$ to this range we carried out a series of hydrocode simulations between ice bodies in the gravity regime using the parallel, smoothed-particle hydrodynamics (SPH)-based code `SPHERAL` [*Owen et al.*, 1998; *Owen*, 2010, 2014]. We simulated impacts into targets with $R = 500$ km and $R = 1000$ km. Target and impactor materials were modeled with a Tillotson equation of state using parameters suitable for H_2O ice [*Melosh*, 1989]. For each target we ran impacts with several specific energies, and for each value of specific energy we used two impactors ($r_i = 250$ km and $r_i = 200$ km) with different velocities, in order to verify velocity-independent scaling. Fitting a line to the remaining bound mass fraction versus the specific impact energy, we thus determine Q_D^* ($R = 500$ km) and Q_D^* ($R = 1000$ km). Figure 1 shows these values next to values obtained previously for smaller targets by *Benz and Asphaug* [1999, Figure 4], demonstrating a very good agreement between the different codes. (For more detail about the SPH simulations, see the supporting information.)

We find that for ice targets in the gravity regime, Q_D^* is well approximated by

$$Q_D^* \approx 0.05\ \mathrm{J/kg} \times \left(\frac{R}{1\ \mathrm{m}}\right)^{1.188}. \tag{2}$$

The above scaling law is valid for head-on impacts. Oblique impacts can be handled by considering only the fraction of impactor volume that intersects the target [*Asphaug*, 2010; *Leinhardt and Stewart*, 2012].

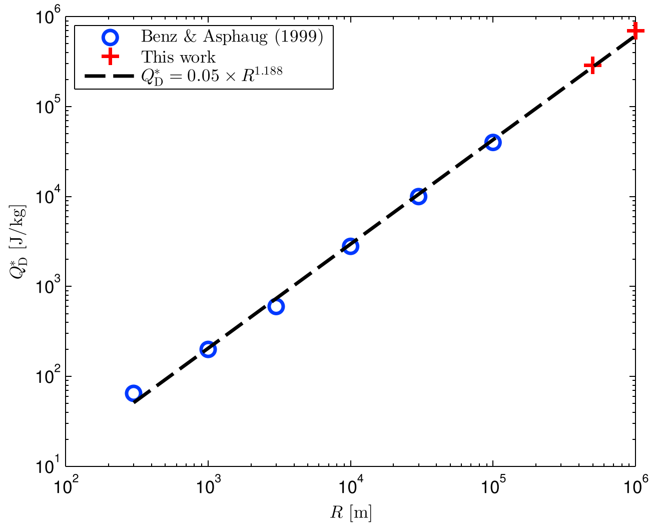

Figure 1. Impact energy required to disperse half the mass (Q^*_D) from an ice target in a gravity-dominated collision as a function of target radius (R) obtained from SPH simulations.

Consider, for example, Mimas, the innermost satellite of Saturn. It has a radius of ∼200km and a mass of ∼3.8×10^{19} kg. By equation (2), $Q^*_D \approx 10^5$ J/kg. In order of magnitude, the impact velocity of a heliocentric impactor is the satellite's orbital velocity, $v_{\mathrm{orb}} \approx 14$ km/s. A single 20 km radius ice impactor at this velocity carries enough energy to disperse half the satellite's mass. In the nominal Nice model, Mimas is expected to encounter a total impactor mass equivalent to hundreds of such bodies.

In the high-energy but relatively low-velocity impacts simulated here, the ejected mass is not vaporized. This is not surprising, since significant shock-induced melting and vaporization of ice require impact velocities higher than ∼8 km/s [*Kraus et al.*, 2011]. In our numerical simulations it was necessary to use lower (but still supersonic) impact velocities so that a higher impactor-to-target size ratio can be used—a requirement of numerical resolution. In reality some vapor production is bound to occur, but most of the mass ejected by the impact will be in the form of large, solid fragments. Unlike vaporized material, these fragments are expected to subsequently reaccrete in relatively short time (see below).

2.3. Impactor Size and Velocity Distribution

The simple calculation shown above neglects some important details that may mitigate the destructive potential of a hypothetical LHB. First, equation (1) assumes a gravity-dominated impact. If much of the mass delivered by the LHB came in the form of very small (<1 km) impactors, we may expect heavy cratering but no significant mass loss from impacts. Second, equation (1) assumes a head-on impact. If much of the delivered mass came in the form of one or two large (comparable to target size) impactors, the angle of impact would play an important role. A chance glancing impact could spend much of the mass budget to minimal effect. We therefore need to consider the statistics of the impactor population.

Third, and the most important, equation (1) predicts the mass of material initially escaping the gravity of the target body, but this material is not necessarily gone for good. Heliocentric impactors hit a satellite at roughly the orbital velocity, $v_{\mathrm{imp}} \approx \sqrt{3}v_{\mathrm{orb}}$. Material is ejected at a range of velocities up to about v_{imp}, while the escape velocity from the primary at the orbital distance of the satellite is $v^P_{\mathrm{esc}} = \sqrt{2}v_{\mathrm{orb}}$. Thus, much of the material that initially escapes the target goes into a similar orbit about the primary and will eventually reaccrete. The timescale for reaccretion depends on the initial spread in semimajor axis given to the ejected material, which in turn depends on the velocity distribution of ejected material [e.g., *Gladman and Coffey*, 2009]. But even a conservative estimate puts the reaccretion time scale at no more than some thousands of orbits. This is much shorter than the likely interval between impacts. As a result, although some mass loss may well occur, the main effect of multiple catastrophic impacts followed by prompt reaccretion will be to disrupt any preexisting structure. We discuss this possibility further in section 4.

2.3.1. Impactor Size Distribution

The Nice model's trans-Neptunian planetesimal disk is thought to be the progenitor of the present-day Kuiper Belt. So the currently observed size distribution in the Kuiper Belt can serve as a good starting point for a derived size distribution of LHB impactors. Here we adopt the size distribution suggested by *Charnoz et al.* [2009], a distribution scaled to match the cratering record on Iapetus and designed to estimate the distribution in the primordial disk. The cumulative fraction N of planetesimals with radius greater than r is assumed to be a power law with two break points:

$$N(r) = \begin{cases} 1, & r < r_{\min}, \\ r_{\min}^{1.5} r^{-1.5}, & r_{\min} < r < 7.5, \\ 7.5\, r_{\min}^{1.5} r^{-2.5}, & 7.5 < r < 100, \\ 750\, r_{\min}^{1.5} r^{-3.5}, & 100 < r. \end{cases} \quad (3)$$

where r is measured in kilometers and $r_{\min}$ is an arbitrarily chosen smallest impactor. For a given total mass in the population, the choice of $r_{\min}$ determines the total number of impactors.

With this size distribution, less than 0.2% of the mass is found in bodies smaller than 1 km in radius, justifying our use of energy scaling in equation (1). However, more than 65% of the mass is found in bodies larger than 100 km, and so we must account for the collision angle.

The implementation of this size distribution is described in full detail in the supporting information.

2.3.2. Impact Velocity Distribution

The probability distribution of impact velocities is described in *Zahnle et al.* [1998] for hyperbolic impactors with isotropic inclinations and making some assumptions about the planetesimals' velocities at infinity.

The collision angle θ can strongly influence the outcome of a collision. If we assume the canonical $\sin 2\theta$ distribution [*Shoemaker and Wolfe*, 1982], the median collision angle is 45°. In oblique impacts between bodies of comparable size, a significant fraction of the impactor volume is sheared off and leaves the scene largely intact. As a result, a significant fraction of the impact kinetic energy is not coupled to the target and should not be included in Q when calculating the mass ejected by the impact. We deal with this by following the same procedure as in *Leinhardt and Stewart* [2012], considering only the fraction of the impactor mass in the volume intersected by the target at impact.

Consider again the case of Mimas, but now assume a 100 km radius impactor. This impactor contains about half the mass the Nice model predicts was delivered to Mimas during an LHB. A head-on impact is easily enough to destroy Mimas many times over. But at an impact angle of 60° only 10% of the impactor volume intersects the target. This effect adds a strong stochastic element to the outcome of an LHB period that we must consider.

2.4. A Monte Carlo Model

For each target of interest, we simulate a series of random LHB events and look at the outcome.

An LHB event is defined by the total mass delivered to the target, M_{LHB}. This is our main control parameter. We draw a random size, velocity, and angle from the distributions discussed above. We calculate Q, the effective specific energy of the impact intersecting the target, and Q_D^* for the target. If $Q > Q_D^*$, we increment a catastrophic impact counter. We also keep track of supercatastrophic ($Q > 2Q_D^*$) and ultracatastrophic ($Q > 3Q_D^*$) impacts to better quantify how much disruption takes place. The procedure is repeated until the total mass delivered by impacts exceeds M_{LHB}. The last impactor may be reduced ad hoc to avoid overshooting the mass limit.

Note that we make the conservative assumption that any ejected mass is quickly reaccreted. The target's mass and radius thus remain constant throughout the simulation. This approach is conservative since if the target were allowed to lose mass between impacts, we would have to adjust its Q_D^* according to equation (2), making it progressively easier to disrupt.

We begin by setting $M_{\mathrm{LHB}}^{\mathrm{sat}}$ for each target scaled to match $M_{\mathrm{LHB}}^{\mathrm{Callisto}} = 3 \times 10^{20}$ kg as suggested by *Barr and Canup* [2010]. Then we scale down the delivered mass until all Saturnian satellites survive their respective LHBs. For each value of M_{LHB} we ran 200 simulations. The resulting statistics are described below.

3. Results

Figure 2 shows the fraction of Monte Carlo runs that included at least one collision with energy greater than 1, 2, or 3 times Q_D^*, for 11 outer solar system satellites. Mimas, Enceladus, Tethys, and Miranda experienced a catastrophic impact in every simulation. In most runs, Mimas, Enceladus, and Tethys experienced *multiple* catastrophic impacts, including impacts with energy several times that required to completely disrupt the target. These satellites would be heavily modified by an LHB no matter what assumptions we make about

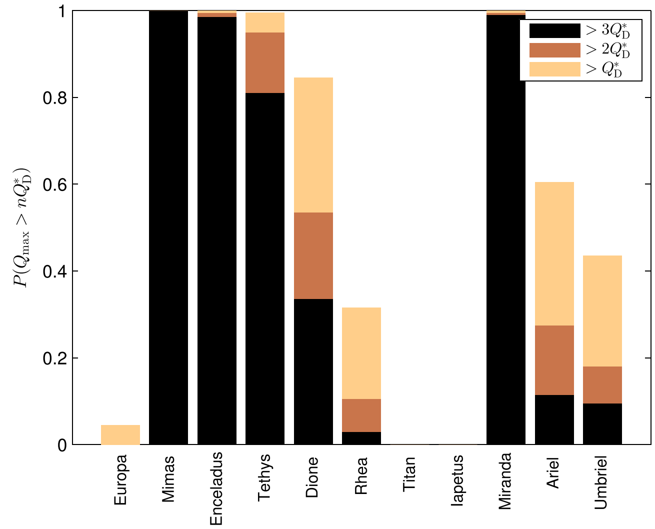

Figure 2. Fraction *P* of Monte Carlo runs that included at least one impact with effective specific energy greater than 1, 2, or 3 times the catastrophic disruption threshold, Q^*_D. In these runs the mass delivered to each satellite was scaled to deliver ~3×10^{20} kg to Callisto [*Barr and Canup*, 2010].

the impactor population or reaccretion efficiency. By contrast, the larger satellites (Europa, Ganymede, Callisto, and Titan) are not expected to undergo disruption nor are very distant objects such as Iapetus.

Figure 3 shows how the probability of catastrophic disruption drops when the total mass delivered in the simulation is reduced. A reduction by a factor of 3 is not enough to save Mimas or Enceladus nor, probably, Tethys or Dione. Figure 3 shows that the mass delivered by a hypothetical LHB must be at least 30 times less than the value predicted by the Nice model to give Enceladus a decent chance of survival and 100 times less to give Mimas any chance at all.

The expected number of destructive events and the overall destruction probabilities calculated in our Monte Carlo simulations are much higher than those previously reported by *Charnoz et al.* [2009, Table 3]. The discrepancy is mainly due to the different values we calculate for the number of impactors larger than a given size expected to hit each satellite. For example, *Charnoz et al.* [2009, Figure 8] calculate that a 200 km satellite at 100,000 km is expected to see about one impact with a 20 km radius comet during the LHB, while a similar body in Mimas orbit is expected to see about 0.57 such comets. In contrast, our Monte Carlo runs, which are scaled from the 3×10^{20} kg striking Callisto, typically result in 30–50 such bodies striking Mimas.

The discrepancy suggests that for a given primordial disk mass, the total mass that we expect to hit all outer planets and their satellites during the LHB is larger than the value calculated by *Charnoz et al.* [2009]. With a primordial disk of 20 Earth masses, the 0.17% probability of impact on Saturn that Charnoz et al. calculate translates to about 2×10^{23} kg striking Saturn, and the relative collision probabilities calculated by *Zahnle et al.* [2003] result in 2.9×10^{19} kg striking Callisto, almost exactly an order of magnitude less than the value suggested by *Barr and Canup* [2010] based on the original Nice model. There may also be other factors contributing to the apparent discrepancy.

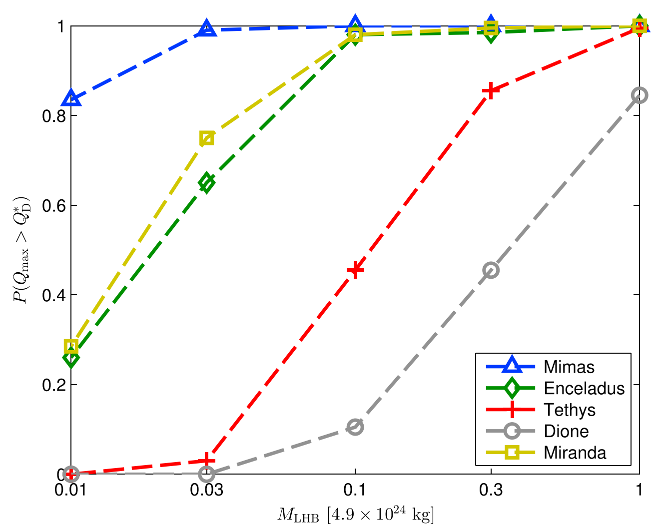

Figure 3. Fraction *P* of simulations that included at least one catastrophic impact, as a function of total mass delivered. The upper limit value corresponds to 3×10^{20} kg delivered to Callisto.

3.1. Caveats

The results given above were obtained using the specific scaling law for Q^*_D, equation (2). This scaling law was derived with hydrocode simulations of impacts, where the equation of state (EOS) plays an important role. We chose to use the Tillotson EOS [*Melosh*, 1989] because it was the easiest to implement in our code, not because it is the best available EOS for ice in the pressure and temperature regime of interest [*Senft and Stewart*, 2008]. Our simulations were also focused on ice targets: the parameters given to the Tillotson EOS were those appropriate for ice [*Melosh*, 1989]. Real targets are

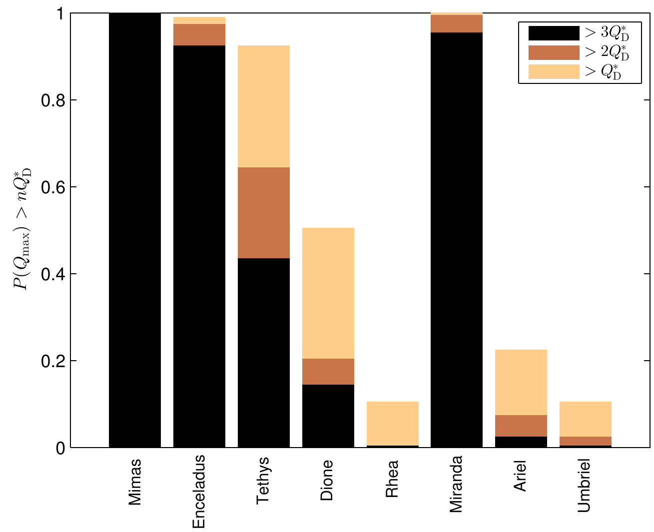

Figure 4. Same as Figure 2 but from runs using a Q^*_D scaling law derived for basalt targets (see text for details).

likely a mix of ice and silicates, but an appropriate EOS for an unknown mixture of H_2O/SiO_2 is difficult to construct.

To verify the robustness of our results in light of the above caveats, we ran several Monte Carlo simulations using a different scaling law. From values given by *Benz and Asphaug* [1999, Figure 3] for basalt targets, we fit

$$Q^*_D \approx 1.48 \text{ J/kg} \times \left(\frac{R}{1 \text{ m}}\right)^{0.9893}. \quad (4)$$

For the targets we are interested in, equation (4) yields values that are about an order of magnitude greater than equation (2). Given the mixed composition of most satellites, we may assume that the two end members, equation (2) for pure ice and equation (4) for pure basalt, bracket the real Q^*_D value for any target.

Running our simulated LHBs with this upper limit Q^*_D, we find that the probability of many satellites' experiencing a catastrophic impact remains high. In particular, as shown in Figure 4, Mimas, Enceladus, Tethys, and Miranda still experience a catastrophic impact in almost every run.

Different scaling laws for gravity regime impacts also exist. *Leinhardt and Stewart* [2012, hereafter LS12] suggest a velocity-dependent scaling law that increases the disruption threshold for high-velocity impacts. The LS12 scaling, however, was based on simulated collisions with targets up to 100 km in radius and does not agree with our SPH simulations of impacts into larger targets. Nevertheless, we ran our Monte Carlo simulation using the LS12 scaling as well. As expected, the total number of catastrophic collisions experienced by each target was reduced. But the probability of experiencing at least one such collision remained almost as high as in our baseline case, so our conclusions given in the following section hold with either scaling law. A direct comparison is shown in the supporting information.

4. Implications

Figures 2 and 3 suggest that the inner Saturnian and Uranian satellites were disrupted (and then reaccreted) several times during the putative LHB. Here we enumerate several consequences of this scenario.

1. The impact history recorded by these satellites prior to the LHB was erased. This conclusion is not in conflict with existing constraints on surface ages based on cratering rate calculations [*Zahnle et al.*, 2003]. In striking contrast, Iapetus—which is not predicted to undergo disruption—has an anomalously large number of impact basins [*Dones et al.*, 2009], perhaps reflecting a contribution from the pre-LHB bombardment not recorded in the inner Saturnian satellites. The ancient surface ages inferred for Callisto, Umbriel, and Oberon are also consistent with our results, since these bodies are not expected to have undergone disruption. Pluto and Charon may likewise have old surface ages, their distant orbit, large size, and low gravitational potential making them immune to any LHB.
2. Catastrophic disruption and prompt reaccretion is likely to lead to a "scrambled" body in which ice and rock are randomly distributed and to initially high levels of porosity. For midsized satellites, neither the energy of reaccretion nor long-lived radioactive decay is sufficient to cause melting and subsequent differentiation [*Monteux et al.*, 2014; *Nagel et al.*, 2004]. Later differentiation could have occurred due to tidal heating (e.g., Enceladus [*Meyer and Wisdom*, 2007], Tethys [*Chen and Nimmo*, 2008], perhaps Miranda [*Dermott et al.*, 1988]), while later impacts would have added ice-rich material to the surface. Nonetheless, the LHB implies that the interiors of Mimas and (perhaps) Miranda are largely undifferentiated. This prediction is potentially testable, because shape or gravity measurements can under certain circumstances

be used to derive a body's moment of inertia [*Dermott and Thomas*, 1988]. The shape of Mimas is non-hydrostatic [*Thomas*, 2010; *Tajeddine et al.*, 2014], which indicates a relatively cold, stiff body, but does not permit the moment of inertia to be inferred. The shape of Miranda is too uncertain to provide useful information [*Thomas*, 1988].

Deep initial porosity will be removed by compression over time. However, even on tidally heated bodies like Enceladus, there will be a cold, near-surface layer, tens of kilometers thick, in which porosity can survive [e.g., *Besserer et al.*, 2013]. Inactive bodies such as Mimas could potentially have a thicker porous layer, thereby reducing their bulk density.

3. Although our calculations assume complete reaccretion in order to be conservative, collisions are stochastic and some will surely result in mass loss. In particular, for target bodies that are differentiated, the catastrophic collisions which occurred during the LHB are likely to have affected the ice-to-rock ratio. For instance, the apparently ice-rich nature of Tethys can readily be explained if Tethys is a spall fragment produced during a giant impact on a differentiated body [*Asphaug and Reufer*, 2013; *Sekine and Genda*, 2012]. The satellites that we see today may in some cases be fragments of their former selves.
4. We have implicitly assumed that the satellites formed at the same time as the rest of the solar system, i.e., prior to the LHB. One way of avoiding disruption is to posit that the inner satellites formed during or after the LHB. *Charnoz et al.* [2011] and *Crida and Charnoz* [2012] suggest that the midsized moons of Saturn could have been formed by accretion from a massive, ice-rich ring [*Canup*, 2010] containing large silicate fragments. This scenario is consistent with a late (post-LHB) formation of the inner Saturnian satellites and predicts a differentiated Mimas. Indeed, post-LHB satellite formation is a natural outcome if the ring progenitor itself was delivered (or disrupted) by the LHB.

5. Conclusions

The canonical Nice model scenario for the LHB [*Gomes et al.*, 2005] will have caused multiple catastrophic disruption and prompt reaccretion of many outer solar system satellites, particularly Mimas, Enceladus, Tethys, and Miranda. None of these bodies (unlike, say, Iapetus or Callisto) will have recorded any events on their surface prior to 3.9 Ga. The interior structures of Enceladus, Tethys, and Miranda may have been affected by subsequent tidal heating events, but the internal structure of Mimas is predicted to be a scrambled, largely undifferentiated jumble of rock and ice. If Mimas turns out to possess these characteristics, then that will provide strong evidence for the scenario outlined here. Conversely, if Mimas turns out to be a differentiated body, then either a heat source postdating 3.9 Ga capable of causing differentiation but not surface tectonics has to be invoked or Mimas is younger than 3.9 Ga or the Nice model explanation for the LHB—when applied to the outer solar system—requires further modification [e.g., *Walsh et al.*, 2012].

Acknowledgments
We thank John Chambers, Fred Ciesla, Sébastien Charnoz, and Alessandro Morbidelli for useful conversations. We also thank both reviewers for their helpful comments. D.K. was supported by OPR grant NNX11AM57G. N.M. and E.A. were supported by PG and G grant NNX13AR66G.

The Editor thanks Luke Dones and an anonymous reviewer for their assistance in evaluating this paper.

References

Asphaug, E. (2010), Similar-sized collisions and the diversity of planets, *Chem. Erde*, *70*(3), 199–219, doi:10.1016/j.chemer.2010.01.004.
Asphaug, E., and A. Reufer (2013), Late origin of the Saturn system, *Icarus*, *223*(1), 544–565, doi:10.1016/j.icarus.2012.12.009.
Barr, A. C., and R. M. Canup (2010), Origin of the Ganymede–Callisto dichotomy by impacts during the Late Heavy Bombardment, *Nat. Geosci.*, *3*(3), 164–167, doi:10.1038/ngeo746.
Benz, W., and E. Asphaug (1999), Catastrophic disruptions revisited, *Icarus*, *142*, 5–20.
Besserer, J., F. Nimmo, J. H. Roberts, and R. T. Pappalardo (2013), Convection-driven compaction as a possible origin of Enceladus's long wavelength topography, *J. Geophys. Res. Planets*, *118*, 908–915, doi:10.1002/jgre.20079.
Canup, R. M. (2010), Origin of Saturn's rings and inner moons by mass removal from a lost Titan-sized satellite, *Nature*, *468*(7326), 943–946, doi:10.1038/nature09661.
Charnoz, S., A. Morbidelli, L. Dones, and J. Salmon (2009), Did Saturn's rings form during the Late Heavy Bombardment?, *Icarus*, *199*(2), 413–428, doi:10.1016/j.icarus.2008.10.019.
Charnoz, S., A. Crida, J. C. Castillo-Rogez, V. Lainey, L. Dones, O. Karatekin, G. Tobie, S. Mathis, C. Le Poncin-Lafitte, and J. Salmon (2011), Accretion of Saturn's mid-sized moons during the viscous spreading of young massive rings: Solving the paradox of silicate-poor rings versus silicate-rich moons, *Icarus*, *216*(2), 535–550, doi:10.1016/j.icarus.2011.09.017.
Chen, E. M. A., and F. Nimmo (2008), Implications from Ithaca Chasma for the thermal and orbital history of Tethys, *Geophys. Res. Lett.*, *35*, L19203, doi:10.1029/2008GL035402.
Crida, A., and S. Charnoz (2012), Formation of regular satellites from ancient massive rings in the solar system, *Science*, *338*, 196–1199.
Dermott, S. F., and P. C. Thomas (1988), The shape and internal structure of Mimas, *Icarus*, *73*, 25–65.
Dermott, S. F., M. Renu, and C. D. Murray (1988), Dynamics of the Uranian and Saturnian satellite systems: A chaotic route to melting Miranda?, *Icarus*, *76*, 295–334.
Dones, L., and H. Levison (2013), The impact rate on giant planet satellites during the Late Heavy Bombardment, in *44th Lunar and Planetary Science Conference,* p. 2772, The Woodlands, Tex., 18–22 March.
Dones, L., C. R. Chapman, W. B. Mckinnon, H. Melosh, M. R. Kirchoff, G. Neukum, and K. J. Zahnle (2009), Icy satellites of Saturn: Impact cratering and age determination, in *Saturn From Cassini-Huygens*, edited by M. K. Dougherty, L. W. Esposito, and S. M. Krimigis, pp. 613–635, Springer, Dordrecht, Netherlands, doi:10.1007/978-1-4020-9217-6.

Gladman, B., and J. Coffey (2009), Mercurian impact ejecta: Meteorites and mantle, *Meteorit. Planet. Sci.*, *44*(2), 285–291, doi:10.1111/j.1945-5100.2009.tb00734.x.

Gomes, R., H. Levison, K. Tsiganis, and A. Morbidelli (2005), Origin of the cataclysmic late heavy bombardment period of the terrestrial planets, *Nature*, *435*(7041), 466–469, doi:10.1038/nature03676.

Kraus, R. G., L. E. Senft, and S. T. Stewart (2011), Impacts onto H_2O ice: Scaling laws for melting, vaporization, excavation, and final crater size, *Icarus*, *214*(2), 724–738, doi:10.1016/j.icarus.2011.05.016.

Leinhardt, Z. M., and S. T. Stewart (2012), Collisions between gravity-dominated bodies. I. Outcome regimes and scaling laws, *Astrophys. J.*, *745*(1), 79, doi:10.1088/0004-637X/745/1/79.

Melosh, H. (1989), *Impact Cratering: A Geologic Process*, 245 pp., Oxford Univ. Press, New York.

Meyer, J., and J. Wisdom (2007), Tidal heating in Enceladus, *Icarus*, *188*(2), 535–539, doi:10.1016/j.icarus.2007.03.001.

Monteux, J., G. Tobie, G. Choblet, and M. Le Feuvre (2014), Can large icy moons accrete undifferentiated?, *Icarus*, *237*, 377–387, doi:10.1016/j.icarus.2014.04.041.

Nagel, K., D. Breuer, and T. Spohn (2004), A model for the interior structure, evolution, and differentiation of Callisto, *Icarus*, *169*(2), 402–412, doi:10.1016/j.icarus.2003.12.019.

Nesvorný, D. (2011), Young solar system's fifth giant planet?, *Astrophys. J.*, *742*(2), L22, doi:10.1088/2041-8205/742/2/L22.

Nesvorný, D., D. Vokrouhlický, and A. Morbidelli (2013), Capture of Trojans by jumping Jupiter, *Astrophys. J.*, *768*, 45, doi:10.1088/0004-637X/768/1/45.

Nimmo, F., and D. Korycansky (2012), Impact-driven ice loss in outer solar system satellites: Consequences for the Late Heavy Bombardment, *Icarus*, *219*(1), 508–510, doi:10.1016/j.icarus.2012.01.016.

Owen, J. (2010), ASPH modeling of material damage and failure, paper presented at 5th International SPHERIC SPH Workshop, pp. 297–304, Manchester, U. K., 23–25 June.

Owen, J. (2014), A compatibly differenced total energy conserving form of SPH, *Int. J. Numer. Methods Fluids*, *75*, 749–775, doi:10.1002/fld.3912.

Owen, J., J. Villumsen, P. Shapiro, and H. Martel (1998), Adaptive smoothed particle hydrodynamics: Methodology II, *Astrophys. J. Suppl. Ser.*, *116*, 155–209.

Sekine, Y., and H. Genda (2012), Giant impacts in the Saturnian system: A possible origin of diversity in the inner mid-sized satellites, *Planet. Space Sci.*, *63–64*, 133–138, doi:10.1016/j.pss.2011.05.015.

Senft, L. E., and S. T. Stewart (2008), Impact crater formation in icy layered terrains on Mars, *Meteorit. Planet. Sci.*, *43*(12), 1993–2013, doi:10.1111/j.1945-5100.2008.tb00657.x.

Shoemaker, E. M., and R. Wolfe (1982), Cratering time scales for the Galilean satellites, in *Satellites of Jupiter*, edited by D. Morrison, pp. 277–339, Univ. of Ariz. Press, Tucson, Ariz.

Smith, B. A., et al. (1982), A new look at the Saturn system: The Voyager 2 images, *Science*, *215*(4532), 504–537, doi:10.1126/science.215.4532.504.

Smith, B. A., et al. (1986), Voyager 2 in the Uranian system: Imaging science results, *Science*, *233*(4759), 43–64, doi:10.1126/science.233.4759.43.

Tajeddine, R., N. Rambaux, V. Lainey, S. Charnoz, A. Richard, A. Rivoldini, and B. Noyelles (2014), Constraints on Mimas' interior from Cassini ISS libration measurements, *Science*, *346*(6207), 322–324, doi:10.1126/science.1255299.

Thomas, P. C. (1988), Radii, shapes, and topography of the satellites of Uranus from limb coordinates, *Icarus*, *73*, 427–441.

Thomas, P. C. (2010), Sizes, shapes, and derived properties of the Saturnian satellites after the Cassini nominal mission, *Icarus*, *208*, 395–401, doi:10.1016/j.icarus.2010.01.025.

Tsiganis, K., R. Gomes, A. Morbidelli, and H. Levison (2005), Origin of the orbital architecture of the giant planets of the solar system, *Nature*, *435*(7041), 459–61, doi:10.1038/nature03539.

Walsh, K. J., A. Morbidelli, S. N. Raymond, D. P. O'Brien, and A. M. Mandell (2012), Populating the asteroid belt from two parent source regions due to the migration of giant planets—"The Grand Tack", *Meteorit. Planet. Sci.*, *47*(12), 1941–1947, doi:10.1111/j.1945-5100.2012.01418.x.

Zahnle, K., L. Dones, and H. Levison (1998), Cratering rates on the Galilean satellites, *Icarus*, *136*(2), 202–22.

Zahnle, K., P. Schenk, H. Levison, and L. Dones (2003), Cratering rates in the outer solar system, *Icarus*, *163*(2), 263–289, doi:10.1016/S0019-1035(03)00048-4.

